

# We are IntechOpen, the world's leading publisher of Open Access books Built by scientists, for scientists

6,900

Open access books available

186,000

International authors and editors

200M

Downloads

Our authors are among the

154

Countries delivered to

TOP 1%

most cited scientists

12.2%

Contributors from top 500 universities



WEB OF SCIENCE™

Selection of our books indexed in the Book Citation Index  
in Web of Science™ Core Collection (BKCI)

Interested in publishing with us?  
Contact [book.department@intechopen.com](mailto:book.department@intechopen.com)

Numbers displayed above are based on latest data collected.  
For more information visit [www.intechopen.com](http://www.intechopen.com)



# Characterization, Photoelectric Properties, Electrochemical Performances and Photocatalytic Activity of the Fe<sub>2</sub>O<sub>3</sub>/TiO<sub>2</sub> Heteronanostructure

*Salah Kouass, Hassouna Dhaouadi, Abdelhak Othmani and Fathi Touati*

## Abstract

The Fe<sub>2</sub>O<sub>3</sub>/TiO<sub>2</sub> nanocomposite was synthesized on FTO substrate via hydrothermal method. The crystal structure, morphology, band structure of the heterojunction, behaviors of charge carriers and the redox ability were characterized by XRD, HR-TEM, absorption spectra, PL, cyclic voltammetry and transient photocurrent spectra. The as-prepared Fe<sub>2</sub>O<sub>3</sub>/TiO<sub>2</sub> photocatalysts with distinctive structure and great stability was characterized and investigated for the degradation of methylene blue (MB) dye in aqueous solution. The ability of the photocatalyst for generating reactive oxygen species, including O<sub>2</sub><sup>-</sup> and ·OH was investigated. It was revealed that the combination of the two oxides (Fe<sub>2</sub>O<sub>3</sub> and TiO<sub>2</sub>) nano-heterojunction could enhance the visible response and separate photogenerated charge carriers effectively. Therefore, the remarkable photocatalytic activity of Fe<sub>2</sub>O<sub>3</sub>/TiO<sub>2</sub> nanostructures for MB degradation was ascribed to the enhanced visible light absorption and efficient interfacial transfer of photogenerated electrons from Fe<sub>2</sub>O<sub>3</sub> to TiO<sub>2</sub> due to the lower energy gap level of Fe<sub>2</sub>O<sub>3</sub>/TiO<sub>2</sub> hybrid heterojunctions as evidenced by the UV-Vis and photoluminescence studies. The decrease of the energy gap level of Fe<sub>2</sub>O<sub>3</sub>/TiO<sub>2</sub> resulted in the inhibition of electron-hole pair recombination for effective spatial charge separation, thus enhancing the photocatalytic reactions. Based on the obtained results, a possible mechanism for the improved photocatalytic performance associated with Fe<sub>2</sub>O<sub>3</sub>/TiO<sub>2</sub> was proposed. The Fe<sub>2</sub>O<sub>3</sub>/TiO<sub>2</sub> nanocomposite has a specific capacity of 82 F.g<sup>-1</sup> and shows a higher capacitance than Fe<sub>2</sub>O<sub>3</sub>.

**Keywords:** Fe<sub>2</sub>O<sub>3</sub>/TiO<sub>2</sub>, methylene blue degradation, heterojunction, holes and superoxide radicals, photocatalyst

## 1. Introduction

The environmental impact caused by the discharge of untreated wastewaters, or even partially treated in sewage stations, is an increasingly worrying problem, considering the damage caused to the environment [1]. In view of this, a great effort

has been made to develop new technologies aiming the treatment of persistent substances in the environment such as heterogeneous photocatalysis, electrochemical techniques and photoelectrochemical processes [2–6]. Among these processes, the heterogeneous photocatalysis that belongs to the class of the advanced oxidation processes has proved very effective as it mineralizes the contaminations existing liquid phases. Over the last few decades, research in the photocatalysis area has been focusing on improving electrochemical and photocatalytic materials [7–10]. So, various photocatalysts such as titanium dioxide ( $\text{TiO}_2$ ) were used. It is one of the most used photocatalysts given its efficiency in pollutant degradation in waste water, because of its inexpensiveness, hard-soluble and long-term photostability. However, there are two defects limiting the use of  $\text{TiO}_2$  in the photocatalysis: one, its wide band gap energy that limits its response to visible light and the other is the rapid recombination of photogenerated electron-hole which leads to the decrease of its photocatalytic activity. Therefore, much effort has been devoted to solving these problems. One solution to overcome the defects is to construct heterojunction photocatalysts. In order to construct a heterojunction photocatalyst based on  $\text{TiO}_2$ , the adaptation of energy levels between the two components is determining, that is, the conduction band edge of the narrow band gap semiconductor is higher than that of  $\text{TiO}_2$ .  $\text{Fe}_2\text{O}_3$ , as a highly active photocatalyst with a band gap of 2.0 eV [11–13], seems to be a good choice except it has a lower conduction band edge. However, the Fermi level ( $E_F$ ) of  $\text{Fe}_2\text{O}_3$  is lower than that of  $\text{TiO}_2$ . Indeed, Yanqing Cong and al. proved that  $\text{Fe}_2\text{O}_3$  nanoparticles present a stronger photo-response under visible light irradiation in the nanostructured  $\text{Fe}_2\text{O}_3/\text{TiO}_2$  nanotube electrodes [14].  $\text{Fe}_2\text{O}_3/\text{TiO}_2$  nanocomposites revealed outstanding photocatalytic activity under visible light and were used as photocatalysts in the degradation of oxytetracycline [15–18]. In this study, we have synthesized by a hydrothermal approach a  $\text{TiO}_2/\text{Fe}_2\text{O}_3$  heterojunction photocatalyst that exhibited excellent performance in many fields.

## 2. Characterization

The XRD analysis of  $\text{Fe}_2\text{O}_3/\text{TiO}_2$  indicates the formation of the  $\text{TiO}_2$  anatase phase in the presence of the  $\text{Fe}_2\text{O}_3$  rhombohedral structure.  $\text{Fe}_2\text{O}_3$  and the  $\text{Fe}_2\text{O}_3/\text{TiO}_2$  nanocomposite were recorded using high resolution transmission electron microscope (HR-TEM). As shown in **Figure 1a**, the  $\text{Fe}_2\text{O}_3$  nanorods are well dispersed with an average diameter of 50 nm.

The magnified high resolution TEM image (**Figure 1a**) illustrates that the  $\text{Fe}_2\text{O}_3$  nanorods cover the  $\text{TiO}_2$  nanoparticles surface. Lattice fringes in the HRTEM image (**Figure 1b**) of the binary hybrid nanocomposite  $\text{Fe}_2\text{O}_3/\text{TiO}_2$  could be assigned to a lattice spacing of 2.35 Å nm corresponding to the (103) plane of  $\text{TiO}_2$ , while the lattice spacing of 2.52 Å nm could be indexed to the (110) plane of  $\text{Fe}_2\text{O}_3$ .

The band gap ( $E_g$ ) for pure  $\text{Fe}_2\text{O}_3$ ,  $\text{TiO}_2$  and the  $\text{Fe}_2\text{O}_3/\text{TiO}_2$  is determined by extrapolating the absorption edge using the following Equation [19]:

$$(\alpha h\nu)^2 = A(h\nu - E_g) \quad (1)$$

The  $E_g$  values are respectively,  $E_{g1} = 3.1$  eV,  $E_{g2} = 1.93$  eV and  $E_{g3} = 2.6$  eV for  $\text{TiO}_2$ ,  $\text{Fe}_2\text{O}_3$  and  $\text{Fe}_2\text{O}_3/\text{TiO}_2$  junction. It is noted that the presence of  $\text{Fe}_2\text{O}_3$  in the material increases the intensity of the bands and shifting them to higher wavelengths compared to  $\text{TiO}_2$ .

Introducing an appropriate amount of transition metal oxide in the  $\text{TiO}_2$  matrix is a promising alternative used to modulate the band gap of the as-obtained

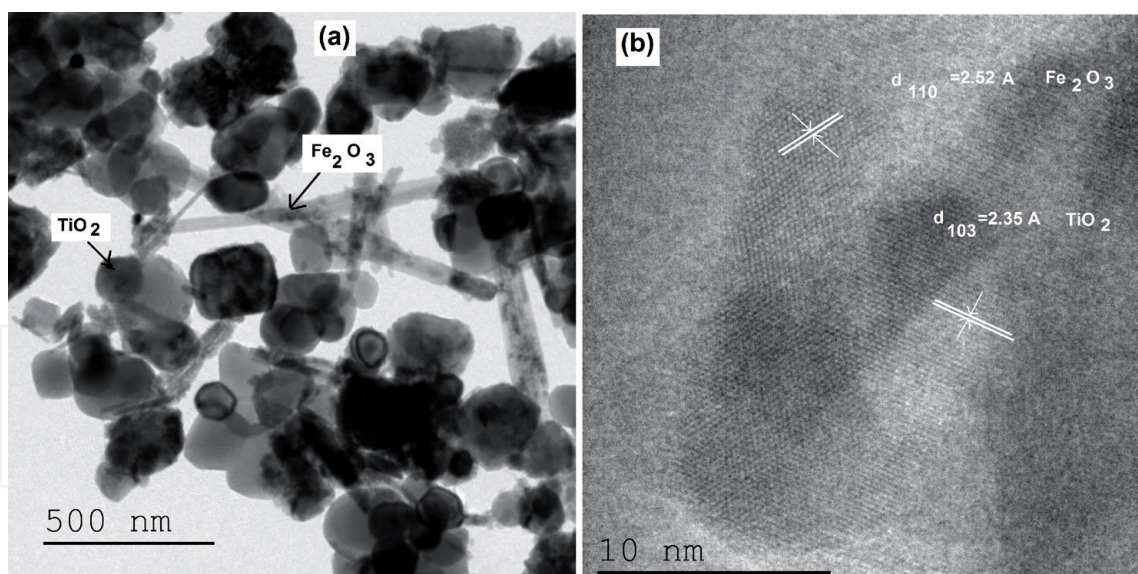


**Figure 1.**  
 HRTEM image of: (a)  $\text{Fe}_2\text{O}_3/\text{TiO}_2$ , (b) HRTEM lattice fringe image of:  $\text{Fe}_2\text{O}_3/\text{TiO}_2$ .

nanocomposite. The weakness of band gap due to the electrons excited and injected into the conduction band of  $\text{TiO}_2$  leads to the improvement of the electron–hole pair separation. The higher degradation activity of the nanocomposite samples ( $\text{Fe}_2\text{O}_3/\text{TiO}_2$ ,  $\text{CdO}/\text{ZnO}$ ,  $\text{ZnO}/\text{TiO}_2$ ,  $\text{Bi}_2\text{O}_3/\text{TiO}_2$  and  $\text{CdS}/\text{TiO}_2$ ) [19–24] is correlated with its lower band gap and strong adsorption in the visible region. In our case, the synthesized  $\text{Fe}_2\text{O}_3/\text{TiO}_2$  heterojunction presents a moderate band gap ( $E_g = 2.6 \text{ eV}$ ) compared to the other nanocomposite samples. Consequently, the separation efficiency of photogenerated electron–hole pairs in the  $\text{Fe}_2\text{O}_3/\text{TiO}_2$  heterojunction could be improved, leading to the improvement of the photocatalytic activity.

### 3. Photocatalytic activity

The study of the photocatalytic activity of  $\text{Fe}_2\text{O}_3/\text{TiO}_2/\text{FTO}$  heterojunction is realized by following the degradation of MB in an aqueous solution under visible light irradiation. The absorption spectrum of MB without a catalyst is characterized by a broad peak centered at 670 nm. The MB absorbance at around 650 nm decreases and there is almost no shift in the peak maximum. This shows that MB was degraded via the destruction of the conjugated structure. This demonstrates that  $\text{Fe}_2\text{O}_3/\text{TiO}_2/\text{FTO}$  exhibits outstanding photocatalytic activity compared to pure  $\text{TiO}_2$ . The obtained results confirm that  $\text{TiO}_2$  alone is unable to absorb under visible irradiation. This could be attributed to the scaling down of the distance between the valence band (VB) and the conduction band (CB) after the addition of  $\text{Fe}_2\text{O}_3$  which boosts the transfer of electrons between bands after excitation. In comparison, the  $\text{Fe}_2\text{O}_3/\text{TiO}_2/\text{FTO}$  exhibits better photocatalytic degradation than the  $\text{TiO}_2$  film. Photocatalytic activity is controlled by many factors, such as the phase structure, particle size, light absorption capacity and electron/hole recombination rate [25].

The heterogeneous photocatalysis mechanism has been discussed extensively in the literature [26, 27]. The photo-activity mechanism presented in this study of the  $\text{Fe}_2\text{O}_3/\text{TiO}_2$  thin film is described as follows: when the system is irradiated with visible light, the  $\text{Fe}_2\text{O}_3$  electrons at the valence band are excited and hop to the conduction band, leaving a hole ( $h^+$ ). As a result, electron ( $e^-$ )/hole ( $h^+$ ) pairs are forming. Then, the excited-state electrons produced by  $\text{Fe}_2\text{O}_3$  can be transferred to the conduction band (CB) of the coupled  $\text{TiO}_2$  due to the existence of electric fields



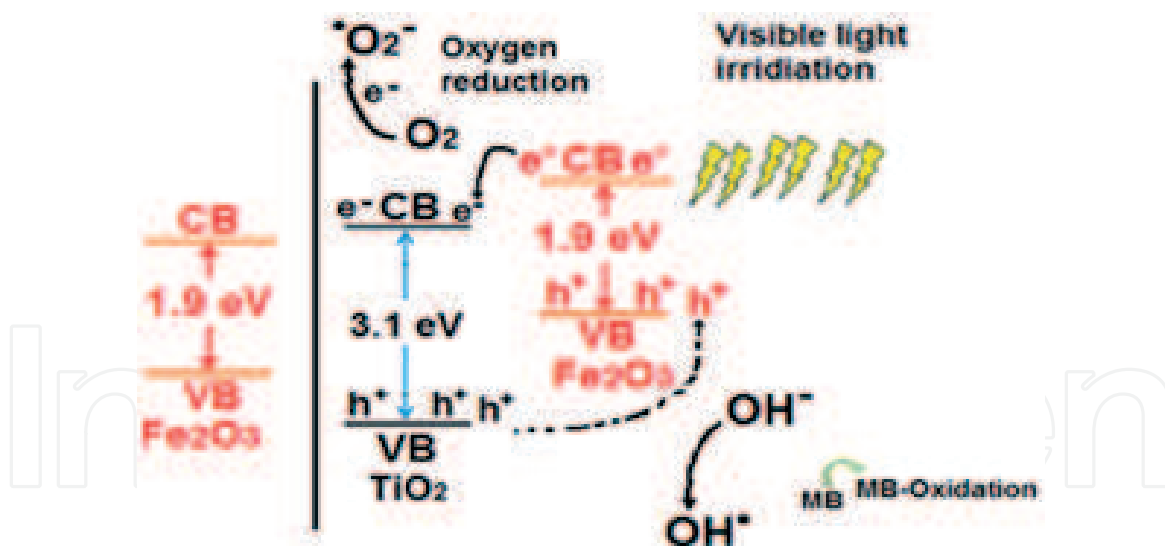


**Figure 2.**

*Schematic illustration of the MB degradation mechanism, under visible light irradiation on the surface of the  $\text{Fe}_2\text{O}_3/\text{TiO}_2/\text{FTO}$  heterojunction.*

between the two materials. At the same time, the photo-generated holes ( $h^+$ ) of  $\text{TiO}_2$  can quickly transfer to the VB of  $\text{Fe}_2\text{O}_3$ . The transferred electrons into the conduction band of  $\text{TiO}_2$  react with dissolved ( $\text{O}_2$ ) to form ( $\cdot\text{O}_2^-$ ) and further produce  $\cdot\text{OH}$ . On the other hand, the holes generated on the valence band of  $\text{Fe}_2\text{O}_3$  can easily transfer to that of  $\text{TiO}_2$  inducing an effective charge separation and transfer. Then the positive charge hole ( $h^+$ ) on  $\text{Fe}_2\text{O}_3$  surfaces reacts with  $\text{H}_2\text{O}$  to generate  $\text{OH}$ .

**Figure 2** shows the band gap structure and the possible charge carrier transfer between  $\text{Fe}_2\text{O}_3$  and  $\text{TiO}_2$  under visible light radiation. Before the contact between the two materials, the conduction band (CB) of  $\text{TiO}_2$  lies above the CB of  $\alpha\text{-Fe}_2\text{O}_3$ . The energy values of VB ( $\text{Fe}_2\text{O}_3$ ) and CB ( $\text{TiO}_2$ ) were obtained by the two formulas:  $E_{\text{VB}} = \chi - E_e + 0.5E_g$  and  $E_{\text{CB}} = E_{\text{VB}} - E_g$ . [28–30], where  $E_g$ ,  $E_e$  and  $\chi$  represent the band gap energy of the semiconductor, the energy of free electrons (about 4.5 eV) and the electronegativity of the semiconductor, respectively. The  $\chi$  values for  $\text{TiO}_2$  and  $\text{Fe}_2\text{O}_3$  are 5.83 eV and 5.88 eV, respectively [19]. After substituting  $\chi$  into the equation, the  $E_{\text{VB}}$  of  $\text{TiO}_2$  and  $\text{Fe}_2\text{O}_3$  are found to be 2.93 eV and 2.35 eV, respectively. Therefore, the CB potentials of  $\text{TiO}_2$  and  $\text{Fe}_2\text{O}_3$  were calculated to be (−0.27 eV) and (0.4 eV), respectively. After coupling  $\text{TiO}_2$  with  $\text{Fe}_2\text{O}_3$  to form the p-n heterojunction, the Fermi level of  $\text{Fe}_2\text{O}_3$  was dragged upwards, while the Fermi level of  $\text{TiO}_2$  was dragged downwards, until they were at the same level and reached equilibrium [31, 32].

#### 4. Photoelectric properties

The PL spectrum is one of efficient approaches to depict the recombination efficiency of photogenerated electron–hole pairs through their different intensities [33]. When the photo-induced electrons and holes are easier to recombine and the lifetime of the photogenerated electrons is shorter, and correspondingly the fluorescence intensity is higher. It is obvious that the PL emission intensity of  $\text{Fe}_2\text{O}_3/\text{TiO}_2$  is lower than that of  $\text{TiO}_2$ , implying that the coupling of  $\text{TiO}_2$  and  $\text{Fe}_2\text{O}_3$  can effectively inhibit the recombination of the photo-generated electron–hole pairs. The decrease recombination rate would be more beneficial for many photocatalyst performance enhancement than  $\text{TiO}_2$  [34].

**Figure 3** shows the transient photocurrent spectra for  $\text{TiO}_2$  and  $\text{Fe}_2\text{O}_3/\text{TiO}_2$  samples. As shown in **Figure 3**, the maximum photocurrent density of the  $\text{Fe}_2\text{O}_3/\text{TiO}_2/\text{FTO}$

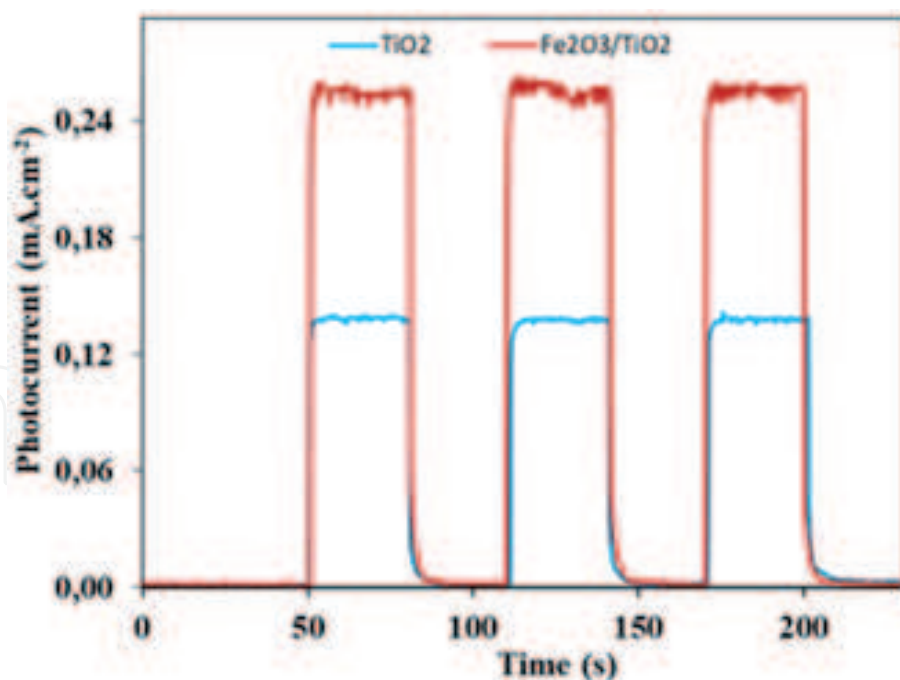


**Figure 3.**  
 Transient photocurrent vs. irradiation time for pure  $\text{TiO}_2$  and  $\text{Fe}_2\text{O}_3/\text{TiO}_2$  heterojunction samples in 0.1 M NaOH solution under visible light irradiation.

heterojunction electrode reached  $0.25 \text{ mA.cm}^{-2}$  which is almost the twice of the pure  $\text{TiO}_2$  electrode. This indicates more charge carriers are generated and transferred from conduction band of the photocatalysts to the electrodes. It could be seen that the photocurrent density produced instantly and increased sharply when exposed to visible light, but promptly reduced to zero as soon as the light source is turned off. Those results confirm that  $\text{Fe}_2\text{O}_3/\text{TiO}_2$  heterojunction is more effective in generating and separating the photogenerated charge carriers than  $\text{TiO}_2$ , and much faster interfacial charge transfer, benefitting photocatalytic activity.

The improved photocurrent shows the effective interfacial charge transfer between  $\text{Fe}_2\text{O}_3$  and  $\text{TiO}_2$ . Thus, the stable and enhanced photocurrent of the obtained heterojunction is more favorable for photocatalytic dye degradation; furthermore, it is more efficient for water splitting [18].

From the resulting Mott-Schottky plot ( $C^{-2}$  versus the applied potential  $E$ ) [35], the flat band potential  $E_{\text{FB}}$  could be obtained as the intercept with the  $x$ -axis and from the slope of the linear part. The value of the flat band potential determined from capacitance measurements is reported to be  $-0.45 \text{ V}$  and  $-0.55 \text{ V}$  vs. Ag/AgCl for  $\text{TiO}_2$  and  $\text{Fe}_2\text{O}_3/\text{TiO}_2$  respectively. It should be noted that the  $E_{\text{FB}}$  of the  $\text{Fe}_2\text{O}_3/\text{TiO}_2$  photoanode exhibits a positive shift in comparison to that of the pure  $\text{TiO}_2$  electrode. Combined with the  $E_g$  calculated from the DRS spectra, the optical band gaps of  $\text{TiO}_2$  and  $\text{Fe}_2\text{O}_3/\text{TiO}_2$  are 3.1 and 2.6 eV, respectively. According to the formula  $E_g = E_{\text{VB}} - E_{\text{CB}}$ , the valence band positions ( $E_{\text{VB}}$ ) of  $\text{TiO}_2$  and  $\text{Fe}_2\text{O}_3/\text{TiO}_2$  are 2.65 and 2.05 V vs. Ag/AgCl, respectively.

## 5. Electrochemical performances

Transition metal oxides such as oxides of Fe, Cu, Ni, Mn, Cu, and  $\text{TiO}_2$  for electrode materials offer rich redox reactions such as in electrochemical cells providing high specific capacitance values for supercapacitors [36, 37]. Among these metal oxides,  $\text{Fe}_2\text{O}_3$ ,  $\text{TiO}_2$ , metal doped  $\text{TiO}_2$  and composite  $\text{Fe}_2\text{O}_3/\text{TiO}_2$  are very promising electrodes materials, due to their acceptable charge/discharge

capacities [38–40]. Cycling stability and specific capacitance are critical factors in evaluating the electrochemical properties, influenced by synthesis method, morphology and grains size.

The specific capacitance of the electrode calculated from the CV curves, according to the following Equation [40–42]:

$$C = \frac{\int I(V)d(V)}{mv\Delta V} \quad (2)$$

$\alpha$ -Fe<sub>2</sub>O<sub>3</sub> with rod-like structure is synthesized to evaluate as electrode material comparing with Cu foil and Ni foam, the as-prepared electrodes with Ni-foam exhibited higher capacity of 415 mAh g<sup>-1</sup> and more stable cycle performance [43]. Fe-based materials, Fe<sub>2</sub>O<sub>3</sub>, Fe<sub>3</sub>O<sub>4</sub>, and FeOOH, were synthesized via the microwave-hydrothermal process by Young Dong Noh and al, the results showed that FeOOH had better anode capacity as lithium-ion batteries than those of Fe<sub>2</sub>O<sub>3</sub> and Fe<sub>3</sub>O<sub>4</sub> [44]. Yudai Huang and al prepared -Fe<sub>2</sub>O<sub>3</sub>/MWCNTs composites by a simple hydrothermal process and show that initial discharge capacity of Fe<sub>2</sub>O<sub>3</sub> is 992.3 mAh g<sup>-1</sup> and the discharge capacity is 146.6 mAh g<sup>-1</sup> after 100 cycles [45].

## 5.1 TiO<sub>2</sub>

Anantha Kumar and al demonstrated that synthesis of a grapheme-TiO<sub>2</sub> using a microwave technique exhibited a high specific capacitance of 165 F g<sup>-1</sup> at a scan rate of 5 mV s<sup>-1</sup> [46]. G. Wang and al fabricate TiO<sub>2</sub>-B nanotubes via a mixed solvothermal technical and subsequent heat treatment and found that specific capacitance is equal to 17.7 F/g [47]. The same, capacitances of the CNTs, CNTs/TiO<sub>2</sub> composite and UVlight irradiated CNTs/TiO<sub>2</sub> composite materials were 4.1F/g; 6.4F/g and 9.8F/g, respectively [48].

## 5.2 TiO<sub>2</sub>-Fe<sub>2</sub>O<sub>3</sub> composite

The performances of TiO<sub>2</sub>-Fe<sub>2</sub>O<sub>3</sub> composite prepared using abundant ilmenite via a heat treatment are improved compared with that of P25, with the increased iron oxide content, the capacity gets higher [49]. Again, the  $\alpha$ -Fe<sub>2</sub>O<sub>3</sub>/TiO<sub>2</sub>/C composite fibers prepared by Luis Zuniga and al, via centrifugal spinning and subsequent thermal processing, showed a superior specific capacity of 340 mAh g<sup>-1</sup> after 100 cycles, compared to 61 mAh g<sup>-1</sup> and 121 mAh g<sup>-1</sup> for TiO<sub>2</sub>/C and  $\alpha$ -Fe<sub>2</sub>O<sub>3</sub>/C materials, respectively [50]. So, TiO<sub>2</sub>/FeTiO<sub>3</sub>@C porous materials, synthesized by carbonizing the mixture of pyrrole with lab-made TiO<sub>2</sub>/Fe<sub>2</sub>O<sub>3</sub>, have a superior capacity of 441.5 mAh g<sup>-1</sup> after 300 cycles, Comparing with TiO<sub>2</sub>, TiO<sub>2</sub>@C, and TiO<sub>2</sub>/Fe<sub>2</sub>O<sub>3</sub> [51]. Also, TiO<sub>2</sub>, Fe<sub>2</sub>O<sub>3</sub> NPs and TiO<sub>2</sub>-Fe<sub>2</sub>O<sub>3</sub> are synthesized via green combustion method with *Aloe Vera* gel as a fuel. Compared to pure TiO<sub>2</sub> and Fe<sub>2</sub>O<sub>3</sub> materials, the composite showed stable electrochemical performance after 1000 cycles, which can be beneficial for rechargeable supercapacitor [52].

Based on the synergy between the two metallic oxides, TiO<sub>2</sub> and Fe<sub>2</sub>O<sub>3</sub>, we have produced Fe<sub>2</sub>O<sub>3</sub>/TiO<sub>2</sub> nanocomposite and heterojunction film via the hydrothermal process. The electrochemical performance of the Fe<sub>2</sub>O<sub>3</sub> and Fe<sub>2</sub>O<sub>3</sub>/TiO<sub>2</sub> nanostructures as potential electrode material for supercapacitors, cyclic voltammetry (CV) tests were performed in a three-electrode cell with Na<sub>2</sub>SO<sub>4</sub> aqueous electrolyte. The current response as a function of the potential applied to the working electrode, recorded at 100 mV/s in a potential range between -0.8 V and -0.4 V with 1000 cycles of the Fe<sub>2</sub>O<sub>3</sub>/TiO<sub>2</sub> nanocomposite in the

Na<sup>+</sup>-system. Therefore, the Fe<sub>2</sub>O<sub>3</sub>/TiO<sub>2</sub> nanocomposite shows electrochemical and structural stability during redox cycling.

The excellent pseudocapacitive performance of the Fe<sub>2</sub>O<sub>3</sub>/TiO<sub>2</sub> nanocomposite electrode is probably attributed to the positive synergistic effects between the Fe<sub>2</sub>O<sub>3</sub> and TiO<sub>2</sub>.

First, This combination can not only inhibit the agglomerating of TiO<sub>2</sub> nanoparticles but also reduce the aggregation of the nanoparticles made the nearly every Fe<sub>2</sub>O<sub>3</sub> nanoparticle access to the electronic and ionic transport pathways resulting in high double-layer capacitance, and importantly, enhancing the utilization of active materials [28]. Second, the large distance between neighboring graphene nanosheets provide enough void spaces to buffer volume change during the redox reaction, and endow good electrical contact with the nanoparticles upon cycling [32, 37]. Third, the unique structure can facilitate the diffusion and migration of the electrolyte ions that can increase the specific capacitance value and improve the high rate charge-discharge performance [38, 39]. Finally, graphene also provides a highly conductive network for electron transport during the charge and discharge processes, thus reducing the polarization of the electrodes [44–46].

## 6. Conclusion

TiO<sub>2</sub>, Fe<sub>2</sub>O<sub>3</sub> hematite nanoparticles and Fe<sub>2</sub>O<sub>3</sub>/TiO<sub>2</sub> nanocomposites were synthesized via a simple hydrothermal process. The photocatalytic activity of the Fe<sub>2</sub>O<sub>3</sub>/TiO<sub>2</sub> nanocomposite was evaluated using the degradation of methylene blue (MB) under sunlight irradiation for pollution prevention. The results proved that the Fe<sub>2</sub>O<sub>3</sub>/TiO<sub>2</sub> heterojunction has a higher removal efficiency of MB and stronger photo-response under visible light irradiation. Compared to both pure TiO<sub>2</sub> and Fe<sub>2</sub>O<sub>3</sub>, the Fe<sub>2</sub>O<sub>3</sub>/TiO<sub>2</sub> photocatalyst have enhanced photocatalytic activity. This improved activity of the heterojunction between the TiO<sub>2</sub> and Fe<sub>2</sub>O<sub>3</sub> nanoparticles results from the improved charge transfer and suppressed electron-hole recombination. We have also compared the photoelectric properties of Fe<sub>2</sub>O<sub>3</sub>/TiO<sub>2</sub> heterogeneous photocatalysts with that of pure TiO<sub>2</sub>. The obtained result demonstrated that the formation of heterojunction between Fe<sub>2</sub>O<sub>3</sub> and TiO<sub>2</sub> was pivotal for improving the separation and thus restraining the recombination of photogenerated electrons and holes, which accounts for the enhancement of photocatalytic activity. The study of the role of the active species on Fe<sub>2</sub>O<sub>3</sub>/TiO<sub>2</sub> confirmed that the crucial active species were both holes and superoxide radicals. The Fe<sub>2</sub>O<sub>3</sub>/TiO<sub>2</sub> sample also showed good stability and reusability, suggesting its potential for water purification applications. Likewise, the visible photogenerated electrons in the obtained heterojunction would provide a feasible route to improve solar water splitting, which will be investigated in further studies. The electrochemical properties of the as-synthesized nanocomposite materials ( $\alpha$ -Fe<sub>2</sub>O<sub>3</sub>/TiO<sub>2</sub>) were evaluated by cyclic voltammetry for 1000 cycles. The  $\alpha$ -Fe<sub>2</sub>O<sub>3</sub>/TiO<sub>2</sub> nanocomposite materials exhibited an enhanced specific discharge capacity compared to Fe<sub>2</sub>O<sub>3</sub> nanomaterials. The as-fabricated hybrid electrodes show an impressive performance as a high-capacity anode for Na<sup>+</sup>-ion batteries.



IntechOpen

## Author details

Salah Kouass<sup>1\*</sup>, Hassouna Dhaouadi<sup>2</sup>, Abdelhak Othmani<sup>3</sup> and Fathi Touati<sup>2</sup>


1 Laboratoire des Matériaux Utiles, INRAP, Technopole Sidi-Thabet, Ariana Tunis, Tunisie

2 Laboratoire Matériaux, Traitement et Analyses, INRAP, Technopole Sidi-Thabet, Ariana Tunis, Tunisie

3 Laboratoire de Physique des Matériaux: Structure et Propriétés, Faculté des Sciences de Bizerte, Université de Carthage, Bizerte, Tunisia

\*Address all correspondence to: koissa2000@yahoo.fr

## IntechOpen

© 2021 The Author(s). Licensee IntechOpen. This chapter is distributed under the terms of the Creative Commons Attribution License (<http://creativecommons.org/licenses/by/3.0>), which permits unrestricted use, distribution, and reproduction in any medium, provided the original work is properly cited. 

## References

- [1] Shahmoradi, B.; Ibrahim, I. A.; Sakamoto, N.; Ananda, S.; Row, T. N. G.; Soga, K.; Byrappa, K.; Parsons, S.; Shimizu, Y.; Dye Degradation Enhanced by Coupling Electrochemical Process and Heterogeneous Photocatalysis, *Environ. Technol.* 31(2010) 1213.
- [2] Benekohal, N. P.; Demopoulos, G. P.; "Electrophoretically self-assembled mixed oxide-TiO<sub>2</sub> nano-composite film structures for photoelectrochemical energy conversion : Probing of charge recombination and electron transport resistances, *J. Power Sources*, 240 (2013) 667.
- [3] Calva-Yanez, J. C.; Rincon, M. E.; de la Fuente, M. S.; Alvarado- Tenorio, G. Structural and photoelectrochemical characterization of MWCNT-TiO<sub>2</sub> matrices sensitized with Bi<sub>2</sub>S<sub>3</sub>; *J. Solid State Electrochem.* 17 (2013) 2633.
- [4] Khataee, A. R.; Zarei, M.; Ordikhani-Seyedlar, R.; Heterogeneous photocatalysis of a dye solution using supported TiO<sub>2</sub> nanoparticles combined with homogeneous photoelectrochemical process: Molecular degradation products, *J. Mol. Catal. A: Chem.* 338(2011)84.
- [5] Ochiai, T.; Fujishima, A.; Photo-electrochemical properties of TiO<sub>2</sub> photocatalyst and its applications for environmental purification *J. Photochem. Photobiol., C*, 13 (2012) 247.
- [6] Zhang, Z.; Wang P., Optimization of photoelectrochemical water splitting performance on hierarchical TiO<sub>2</sub> nanotube arrays; *Energy Environ. Sci.*, 5 (2012) 6506.
- [7] Jinlin Long, Hongjin Chang, QuanGu, Jie Xu, Lizhou Fan, Shuchao Wang, Yangen Zhou, Wei Wei, Ling Huang, Xuxu Wang, Ping Liu, and Wei Huang, Gold-plasmon enhanced solar-to-hydrogen conversion on the {001} facets of anatase TiO<sub>2</sub> nanosheets, *Energ. & Environ. Sci.*, 7(2014) 973-977.
- [8] LingshuMeng, Zhenye Chen, Zhiyun Ma, Sha He, YidongHou, Hao-Hong Li, Rusheng Yuan, Xi-He Huang, Xuxu Wang, Xincheng Wang, Jinlin Long, Gold Plasmon-Induced Photocatalytic Dehydrogenative Coupling of Methane to Ethane on Polar Oxide Surfaces, *Energ. & Environ. Sci.* 11 (2018) 294-298.
- [9] Jie Xu, Liufeng Luo, Guangrui Xiao, Zizhong Zhang, Huaxiang Lin, Xuxu Wang, and Jinlin Long, Layered C<sub>3</sub>N<sub>3</sub>S<sub>3</sub> Polymer/Graphene Hybrids as Metal-Free Catalysts for Selective Photocatalytic Oxidation of Benzylic Alcohols under Visible Light, *ACS Catal.* 4 (2014) 3302-3306.
- [10] C. C. Wang, Y. Zhan and Z. Y. Wang, TiO<sub>2</sub>, MoS<sub>2</sub>, and TiO<sub>2</sub>/MoS<sub>2</sub> Heterostructures for Use in Organic Dyes Degradation, *ChemistrySelect*, 3 (2018) 1713-1718.
- [11] Hongwen Zhang, Lei Ma, Jintao Ming, Bingqian Liu, Yibo Zhao, YidongHou, Zhengxin Ding, Chao Xu, Zizhong Zhang, Jinlin Long, Amorphous Ta<sub>2</sub>O<sub>x</sub>N<sub>y</sub> Enwrapped TiO<sub>2</sub> Rutile Nanorods for Enhanced Solar Photoelectrochemical Water Splitting, *Applied Catalysis B: Environmental* 243 (2019) 481-489.
- [12] R.L. Spray, K.J. McDonald, K.S. Choi, Enhancing photoresponse of nanoparticulate alpha-Fe<sub>2</sub>O<sub>3</sub> electrodes by surface composition tuning, *J. Phys. Chem C*. 115 (8) (2011) 3497-3506.
- [13] A. Umar, M. Abaker, M. Faisal, S.W. Hwang, S. Baskoutas, S.A. Al-Sayari, High-yield synthesis of well-crystalline alpha-Fe<sub>2</sub>O<sub>3</sub> nanoparticles: structural, optical and photocatalytic properties, *J. Nanosci. Nanotechnol.* 11 (4) (2011) 3474-3480.
- [14] Y. Cong, Z. Li, Z. Yi, W. Qi, X. Qian, Synthesis of α-Fe<sub>2</sub>O<sub>3</sub>/TiO<sub>2</sub> nanotube arrays for photoelectro-

- Fenton degradation of phenol, Chem. Engin. J. 191(2012) 356-363.
- [15] L.Rong, J.Yuefa, W. Jun, Z.Qiang, Photocatalytic Degradation and Pathway of Oxytetracycline in Aqueous Solution by  $\text{Fe}_2\text{O}_3/\text{TiO}_2$  Nanopowders, RSC Advances. 51(2015) 1-9.
- [16] M. Ni, M. K. H. Leung, D.Y.C. Leung, K. Sumathy, A review and recent developments in photocatalytic water-splitting using  $\text{TiO}_2$  for hydrogen production, Renew. Sustain. Energy Rev. 11 (2007) 401-425
- [17] J. Tang, J.R. Durrant, D.R. Klug, Mechanism of photocatalytic water splitting in  $\text{TiO}_2$  reaction of water with photoholes, importance of charge carrier dynamics, and evidence for four-hole chemistry, J. Am. Chem. Soc. 124 (2002) 13885-13891.
- [18] P. Luan, M. Xie, X. Fu, Y. Qua, X. Sun, L. Jing, Improved photoactivities of  $\text{TiO}_2/\text{Fe}_2\text{O}_3$  nanocomposites for visible-light water splitting after phosphate bridging and mechanism, Phys. Chem. Chem. Phys. 17 (2015) 5043-5050.
- [19] C. Wei, Z.Maojin, R.Xiaosai, M. Andrew, Synthesis and Photocatalytic Activity of Monolithic  $\text{Fe}_2\text{O}_3/\text{TiO}_2$ , S. Afr. J. Chem. 70(2017) 127-131.
- [20] D. Lee, Y. Rho, F. Allen, A. *minor*, S.H. Ko and C. Grigoropoulos, Synthesis of Hierarchical  $\text{TiO}_2$  Nanowires with Densely-Packed and Omnidirectional Branches, Nanoscale. (2013)
- [21] A Othmani, S. Kouass, Th. Khalfi, S. Bouchada, F. Touati and H. Dhaouadi, Studies of the photocatalytic and electrochemical performance of the  $\text{Fe}_2\text{O}_3/\text{TiO}_2$  heteronanostructure, Journal of the Iranian Chemical Society, <https://doi.org/10.1007/s13738-020-01993-0>.
- [22] J. Tauc, R.Grigorovici, A.Vancu, Optical Properties and Electronic Structure of Amorphous Germanium, Phys. Stat. Sol. 15(1966) 627-637.
- [23] S. Yang, X.Quan, X. Li, Y. Liu, S.Chen, G. Chen, Preparation, characterization and photo-electrocatalytic properties of nanocrystalline  $\text{Fe}_2\text{O}_3/\text{TiO}_2$ ,  $\text{ZnO}/\text{TiO}_2$  and  $\text{Fe}_2\text{O}_3/\text{ZnO}/\text{TiO}_2$  composite film electrodes towards pentachlorophenol degradation, Phys Chem Chem Phys. 6 (2004) 659- 664.
- [24] P.Linlin, X.Tengfeng, L.Yongchun, F.Haimei, W.Dejun, Synthesis, photoelectric properties and photocatalytic activity of the  $\text{Fe}_2\text{O}_3/\text{TiO}_2$  heterogeneous photocatalysts, Phys. Chem. Chem. Phys. 12(2010) 8033-8041.
- [25] L.Yin, Y. Xia, Core-Shell Structured  $\alpha\text{-Fe}_2\text{O}_3@/\text{TiO}_2$  Nanocomposites with Improved Photocatalytic Activity in Visible Light Region, Phys. Chem. Chem. Phys. 15(2013) 1-7
- [26] J. Aslam, M.R. Mohammed, F. Mohammed, B.K. Sher, Studies on Photocatalytic Degradation of Acridine Orange and Chloroform Sensing Using as-Grown Antimony Oxide, Microstructures. Mater. Sc. Appl. 2(2011) 676-683
- [27] L.P. Zhu, N.C. Bing, D.D. Yang, Y. Yang, G.H. Liao, L.J Wang, Synthesis and photocatalytic properties of core-shell structured  $\alpha\text{-Fe}_2\text{O}_3@/\text{SnO}_2$  shuttle-like nanocomposites, Cryst. Eng. Comm. 13 (2011) 4486-4490.
- [28] M.R. Mohammed, M.A. Abdullah, E.Y. Tamer, M.M.Hadi, Photocatalytic degradation of remazol brilliant orange 3R using wet-chemically prepared  $\text{CdO-ZnO}$  nanofibers for environmental remediation, Mater. Express. 6(2016) 137-148.
- [29] W.Liugang, Z.Junying, L.Chunzhi, Z. Hailing, W.Wenwen, W.Tianmin, Synthesis, Characterization and Photocatalytic Activity of  $\text{TiO}_2$  Film/

Bi<sub>2</sub>O<sub>3</sub>Microgrid Heterojunction, J Mater Sci Technol. 27(2011) 59-63.

[30] Z.Panpan, L.Zhanggao, X. Yu, F. Jing, X.Jiangwei, Studies on facile synthesis and properties of mesoporous CdS/TiO<sub>2</sub> composite for photocatalysis applications, J. Alloys. Compounds. 692(2017) 170-177.

[31] L. Peng, T. Xie, Y. Lu, H. Fan, D. Wang, Synthesis, Photoelectric Properties and Photocatalytic Activity of the Fe<sub>2</sub>O<sub>3</sub>/TiO<sub>2</sub> Heterogeneous Photocatalysts, Phys. Chem. Chem. Phys. 12(2010) 8033-8041.

[32] M.Niu, F. Huang, L. Cui, P. Huang, Y. Yu, Y.Wang, Hydrothermal Synthesis, Structural Characteristics, and Enhanced Photocatalysis of SnO<sub>2</sub>/α-Fe<sub>2</sub>O<sub>3</sub> Semiconductor Nanohetero-structures, ACS.Nano. 4(2010) 681-688.

[33] Cong Y., Zhang J., Chen F., Anpo, M. J. Phys. Chem. C, 111 (2007) 6976-6982.

[34] S.D. Deldkar, H.M. Yadav, S.N. Achary, S.S. Meena and S.H. Pawar, Structural refinement and photocatalytic activity of Fe-doped anatase TiO<sub>2</sub> nanoparticles, Appl. Surf. Sci. 263 (2012) 536-545.

[35] Z. Chen, H. N. Dinh and E. Miller, Photoelectrochemical water splitting, Springer Briefs in Energy, New York, (2013) 49-61.

[36] X. Zhang, P. Suresh Kumar, V. Aravindan, H.H. Liu, J. Sundaramurthy, S.G. Mhaisalkar, H.M. Duong, S. Ramakrishna, S. Madhavi, Electrospun TiO<sub>2</sub>—Graphene Composite Nanofibers as a Highly Durable Insertion Anode for Lithium Ion Batteries, J. Phys. Chem. C 116 (2012) 14780-14788.

[37] L. Zuniga, V. Agubra, D. Flores,; H. Campos J. Villareal, M. Alcoutlabi, Multichannel hollow structure for improved electrochemical performance of TiO<sub>2</sub>/Carbon composite nanofibers as

anodes for lithium ion batteries, J. Alloys Compd. 686(2016) 733-743.

[38] L.W. Ji, Z. Lin, M. Alcoutlabi, X.W. Zhang, Recent developments in nanostructured anode materials for rechargeable lithium-ion batteries, Energy Environ. Sci. 4(2011) 2682-2699.

[39] L. Gao, H. Hu, G.J. Li, Q.C. Zhu, Y. Yu, Hierarchical 3D TiO<sub>2</sub>@Fe<sub>2</sub>O<sub>3</sub> nanoframework arrays as high-performance anode materials, Nanoscale 6(2014) 6463-6467.

[40] S. Li, M.Y. Wang, Y. Luo, J.G. Huang, Bio-Inspired Hierarchical Nanofibrous Fe<sub>3</sub>O<sub>4</sub>-TiO<sub>2</sub>-Carbon Composite as a High-Performance Anode Material for Lithium-Ion Batteries. ACS Appl. Mater. Interfaces, 8(2016) 17343-17351.

[41] S.S. Shinde, G.S. Gunda, D.P. Dubal, S.B. Jambure, C.D. Lokhande, Morphological modulation of polypyrrole thin films through oxidizing agents and their concurrent effect on supercapacitor performance, Electrochim. Acta. 119 (2014) 1-10.

[42] D. Qu, H. Shi, Studies of activated carbons used in double-layer capacitors, J. Power. Sources. 74 (1998) 99-107.

[43] L. Huang, Z. Min, Q. Zhang, Research and analysis on electrochemical performances of α-Fe<sub>2</sub>O<sub>3</sub> electrode in Li-ion battery with different current collectors, Materials Research Bulletin 66 (2015) 39-44.

[44] K. Chen, Y. D. Noh, W. Huang, J. Ma, SridharKomarneni, Dongfeng Xue, Microwave-hydrothermal synthesis of Fe-based materials for lithium-ion batteries and supercapacitors. Ceramics International 40 (2014) 2877-2884.

[45] Y. Huang, Z. Dong, D. Jia, Z. Guo d, Won Il Cho, Electrochemical properties of αFe<sub>2</sub>O<sub>3</sub>/MWCNTs as anode materials for lithium-ion batteries, Solid State Ionics 201 (2011) 54-59.



[46] A. Ramadoss, Sang Jae Kim, Improved activity of a grapheme-TiO<sub>2</sub> hybrid electrode in an electrochemical supercapacitor, *CA R B O N* 6 3 (2013) 434-445.

[47] G. Wang, Z.Y. Liu, J.N. Wu, Q. Lu, Preparation and electrochemical capacitance behavior of TiO<sub>2</sub>-B nanotubes for hybrid supercapacitor, *Materials Letters* 71 (2012) 120 122.

[48] Bin Zhang, Rui Shi, Yupeng Zhang, Chunxu Pan, CNTs/TiO<sub>2</sub> composites and its electrochemical properties after UVlight irradiation, *Progress in Natural Science: Materials International* 23(2) (2013)164-169.

[49] Li. Li, J. Zhangb and Q. Zhua, Novel fractional crystallization route to porous TiO<sub>2</sub>-Fe<sub>2</sub>O<sub>3</sub> composites: large scale preparation and high performances as photocatalyst and Li-ion battery anode, *Dalton Trans.* 2015, DOI: 10.1039/C5DT04091D.

[50] Luis Zuniga, Gabriel Gonzalez, Roberto Orrostieta Chavez, Jason C. Myers, Timothy P. Lodge and Mataz Alcoutlabi, Centrifugally Spun  $\alpha$ -Fe<sub>2</sub>O<sub>3</sub>/TiO<sub>2</sub>/Carbon Composite Fibers as Anode Materials for Lithium-Ion Batteries, *Appl. Sci.* 9 (2019) 4032.

[51] S. Guoa, J. Liu, S. Qiu, Y. Wang, X. Yan, N. Wu, S. Wang, Z. Guo, Enhancing Electrochemical Performances of TiO<sub>2</sub> Porous Microspheres through Hybridizing with FeTiO<sub>3</sub> and Nano-carbon, *Electrochimica Acta* 190 (2016) 556-565.

[52] M. R. Anil Kumar, B. Abebe, H. P. Nagaswarupa, H. C. Ananda Murthy, C. R. Ravikumar & Fedlu Kedir Sabir, Enhanced photocatalytic and electrochemical performance of TiO<sub>2</sub>-Fe<sub>2</sub>O<sub>3</sub> nanocomposite: Its applications in dye decolorization and as supercapacitors, *Scientific Reports* 10 (2020) 1249.